

# COMPUTATIONAL STUDY OF CYCLONE FLOW FLUID DYNAMICS USING A DIFFERENT INLET SECTION ANGLE

S. Bernardo<sup>a</sup>,

A. P. Peres<sup>b</sup>,

and M. Mori<sup>c</sup>

<sup>a</sup> UN-SIX / PETROBRAS

A/C: Eng. Sérgio Bernardo - Gerência de Pesquisa

Rodovia BR 476, km 143

Bairro: Vila Prohmann -CEP 83900-000

São Mateus do Sul-PR

<sup>b,c</sup> Universidade Estadual de Campinas

Faculdade de Engenharia Química

Departamento de Processos Químicos

Laboratório de Modelagem e Simulação de

Processos Químicos

Cidade Universitária Zeferino Vaz

Distrito de Barão Geraldo

Caixa Postal 6066, CEP 13083-970

Campinas, São Paulo, Brasil

<sup>a</sup> sergio.BCP\_ENGENHARIA@petrobras.com.br

<sup>b</sup> apperes@lmspq.feq.unicamp.br

<sup>c</sup> mori@feq.unicamp.br

## ABSTRACT

The conventional design of the cyclone model has been used without significant modifications for about a century. Recently, some studies were carried out to improve equipment performance by evaluating the geometric influence of the tangential inlet section and scroll inlet duct design. In this work, the influence of cyclone inlet section geometry was studied using an angle of 45 degrees in relation to the cyclone body. The study was conducted for the gas and gas-particle phases, based on an experimental study available in the literature, where a conventional inlet section was used. Numerical experiments were carried out with the CFX computational code. The fluid dynamics profiles and tangential velocity component were evaluated for three inlet velocities (2.75, 7.75 and 15.2 m/s) using the Reynolds Stress model. The results showed that this proposal is useful for improving the cyclone performance.

**Keywords:** CFD, Cyclones, gas flow, RSM, lean inlet

## INTRODUCTION

The conventional form of cyclone design has survived largely unchanged for over a century. The historical development of the cyclone can be found in Crawford (1976), Storch (1979) and Ogawa (1984), where many old and interesting types of cyclones are discussed. There are various cyclone models in the literature, but the most famous are the Stairmand (1951) and the Lapple (1951) models. These cyclones were developed through experimental tests with the aim of optimizing performance. However, according to Dirgo and Leith (1985), there is no theoretical basis to assure that a specific model has only high performance characteristics.

An important application of the cyclones is the recovery of catalyst in fluid catalytic cracking units (FCCU). The gas cyclone in FCCU is generally used in a multi-cell arrangement to meet recovery requirements of typically more than 99%. At a further stage, a high-efficiency cyclone system may be used to remove the remaining particles. The gas cyclone used at this stage operates at low solids loading, with the particles having a diameter in the range of 0.1-80  $\mu\text{m}$ . High collection

efficiencies (more than 99.9%) are demanded, e.g., to meet environmental regulations on dust emission and/or to prevent excessive wear of turbine blades in energy/recovery systems (Hoekstra et al., 1999).

If the inlet duct is ignored, cyclone geometry is almost axisymmetric and a number of previous Computational Fluid Dynamics (CFD) models have used this feature in order to simplify the model as a two-dimensional case (Duggins and Frith, 1987). While this greatly reduces computational time, a two-dimensional model is limited, since the location of the inlet duct will break flow pattern symmetry. Furthermore, these geometric simplifications cannot be used to assess changes in inlet design or offset vortex finders. The recent increase in computing power and grid generation capabilities has allowed the recent CFD models to include the full three-dimensional geometry and to be used for the evaluation of design modifications.

In this work, a study of the influence of cyclone geometry on an inlet section with a 45 degree angle in relation to the cyclone body is studied. The starting point is based on an experimental study available in the literature (Patterson and Munz, 1989 and 1996), where a

conventional inlet section was used. Also a comparative study with the numerical simulation work of Peres (2002) is conducted. Numerical experiments for a three-dimensional model were carried out for gas and gas-solid flow using CFX, a CFD code available on the market.

**MATHEMATICAL MODELING**

**Turbulence**

Turbulence consists of fluctuations in the flow field in time and space. It is a complex process, mainly because it is three dimensional, unsteady and consists of many scales. It can have a significant effect on the characteristics of the flow. Turbulence occurs when the inertia forces in the fluid become significant compared to viscous forces, and is characterized by a high Reynolds Number. In principle, the Navier-Stokes equations describe both laminar and turbulent flows without the need for additional information. However, turbulent flows at realistic Reynolds numbers span a large range of turbulent length and time scales and would generally involve length scales much smaller than the smallest finite volume mesh which can be practically used in a numerical analysis.

To enable the effects of turbulence to be predicted, a large amount of CFD research has concentrated on methods which make use of turbulence models. Turbulence models have been specifically developed to account for the effects of turbulence without recourse to a prohibitively fine mesh and Direct Numerical Simulation.

**The Reynolds Stress Turbulence Model**

The Reynolds stress turbulence models are based on transport equations for all components of the Reynolds stress tensor and the dissipation rate. These models do not use the eddy viscosity hypothesis, but solve an equation for the transport of Reynolds stresses in the fluid. The Reynolds stress model transport equations are solved for the individual stress components.

The Reynolds averaged momentum equations for the mean velocity U are

$$\frac{\rho \overline{u_i u_j}}{\rho} + \frac{\partial}{\partial x_k} (\overline{u_k u_i u_j}) = P_{ij} + \phi_{ij} + \frac{\partial}{\partial x_k} \left[ \left( \mu + \frac{2}{3} c_s \rho \frac{k^2}{\epsilon} \right) \frac{\partial \overline{u_i u_j}}{\partial x_k} \right] - \frac{2}{3} \delta_{ij} \epsilon \quad (1)$$

where  $p^H$  is a modified pressure,  $m$  is the viscosity,  $B$  is the sum of body forces and the fluctuating Reynolds stress contribution is  $\overline{u \otimes u}$ .

Unlike eddy viscosity models, the modified pressure has no turbulence contribution and is related to the static (thermodynamic) pressure by:

$$p^H = p - 2 \zeta \frac{\partial U}{\partial x} \quad (2)$$

where  $\zeta$  is the bulk viscosity.

In the differential stress model,  $p^H$  has to obey a transport equation. A separate transport equation must be solved for each of the six Reynolds stress components of. The differential equation Reynolds stress transport is:

$$\frac{\partial \rho \overline{u_i u_j}}{\partial t} + \nabla \cdot (\rho \overline{u_i u_j} \otimes U) - \nabla \cdot \left( \rho C \frac{k}{\epsilon} \overline{u_i u_j} (\nabla u \otimes u)^T \right) = P + G + \phi - \frac{2}{3} \delta_{ij} \epsilon \quad (3)$$

where  $P$  and  $G$  are shear and buoyancy turbulence production terms of the Reynolds stresses respectively,  $f$  is the pressure-strain tensor,  $\epsilon$  is dissipation rate of turbulent kinetic energy and  $C$  is a constant.

The differential equations, given bellow, for each component of the Reynolds stresses have been developed and their solution gave each stress component, allowing anisotropy in the turbulent stress terms.

$$\frac{\partial \rho \overline{u_i u_j}}{\partial t} + \frac{\partial}{\partial x_k} (\overline{U_k \rho u_i u_j}) = P_{ij} + \phi_{ij} + \frac{\partial}{\partial x_k} \left[ \left( \mu + \frac{2}{3} c_s \rho \frac{k^2}{\epsilon} \right) \frac{\partial \rho \overline{u_i u_j}}{\partial x_k} \right] - \frac{2}{3} \delta_{ij} \epsilon \quad (4)$$

Here,  $f_{ij}$  is the pressure-strain correlation,  $k$  is turbulent kinetic energy,  $\epsilon$  is dissipation rate of turbulent kinetic energy, and  $P$ , the exact production term, is given by:

$$P = -\rho (\overline{u \cdot u} (\nabla U)^T + (\nabla U) \overline{u \cdot u}) \quad (5)$$

Since the turbulence dissipation appears in the individual stress equations, an equation for  $\epsilon$  is still required:

$$\frac{\partial \rho \epsilon}{\partial t} + \nabla \cdot (\rho U \epsilon) = \frac{\epsilon}{k} (c_{\epsilon 1} P - c_{\epsilon 2} \rho \epsilon) + \nabla \cdot \left[ \frac{1}{\sigma_{\epsilon RS}} \left( \mu + \rho C_{\mu RS} \frac{k^2}{\epsilon} \right) \nabla \cdot \epsilon \right] \quad (6)$$

In these equations, the anisotropic diffusion coefficients of the original models are replaced by an isotropic formulation, which increases the robustness of the RSM. The model constants are:  $C_S = 0,22$ ;  $C_{EI} = 1,45$ ;  $C_{E2} = 1,9$ ;  $C_{MRS} = 0,1152$ .

## NUMERICAL METHODS

Equations were numerically solved by the finite volume method using the commercial CFD code CFX, in which the control volume method is used to discretize the transport equation. The pressure-velocity coupling algorithm SIMPLEC (SIMPLE Consistent Method) and the higher upwind interpolation scheme were used in all numerical experiments. More details on these schemes can be found in Patankar (1980).

### Computational Grid and Boundary Conditions

The cyclone geometry used was based on Patterson and Munz (1996), in which the geometry of the inlet section was modified 45 degrees using an angle in relation to the cyclone body. All geometric configurations are presented in Patterson and Munz (1996). The geometric characteristics of this cyclone and the surface mesh for both cyclones are presented in Fig. 1.

The numerical grids were constructed using the mesh building code ICM CFD HEXA and have around 48000 hexahedral cells. All boundary conditions were based on Patterson and Munz (1989 and 1996) which were used for comparison with the CFD model proposed in this work. Gas flow was assumed to be at Standard Temperature and Pressure (STP) conditions and the inlet velocities used were 2.75, 7.75 and 15.2 m/s. Solid particles were considered to have a 10  $\mu$ m mean diameter and  $\tilde{n} = 2600 \text{ kg/m}^3$ . Solid phase has an inlet volume fraction of  $6.13 \times 10^{-5}$ . The boundary conditions were considered uniform profiles at the inlet for all variables. The conditions at the walls were no slip to gas phase, and free slip to solid phase. Atmospheric pressure conditions were assumed at the outlet.

Peres (2002), where the case studied by Patterson and Munz (1996) was simulated under the same conditions as those used in this work, was used to validate the turbulence model used in the current work.

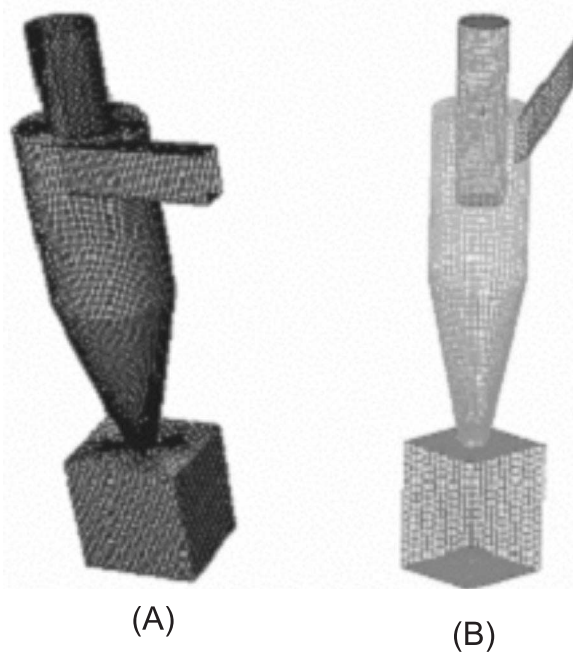


Figure 1. Cyclone geometry and grid for: (A) Patterson and Munz (1989, 1996) and (B) 45 degree angle (current case).

## RESULTS

### Gas Flow Study

Figures 2, 3 and 4 show the numerical solutions obtained for the distributions of tangential velocities of the gas obtained at a height of 0.12 m from the top of the cyclone in the current work.

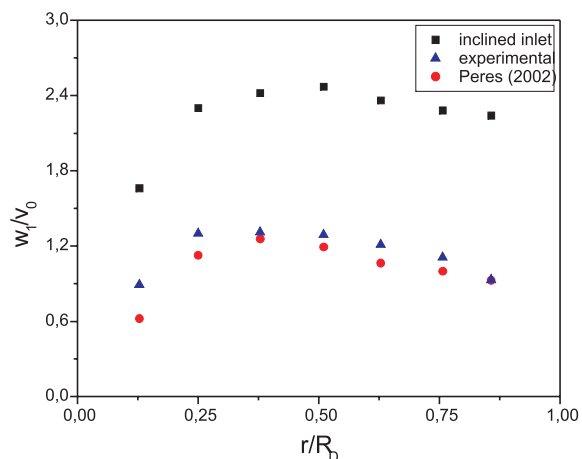


Figure 2. Distributions of tangential velocity in the cyclone ( $v_0 = 2.75 \text{ m/s}$ ).

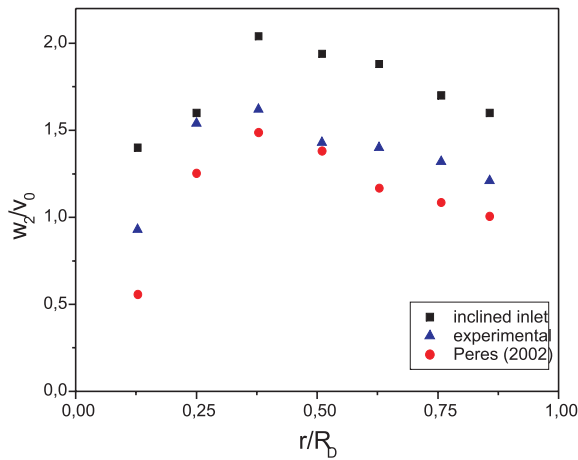


Figure 3. Distributions of tangential velocity in the cyclone ( $v_0 = 7.75$  m/s).

Numerical results provided a good representation of the swirling flow in the cyclone. Data obtained on the capability of the turbulence model to represent the radial distributions of tangential velocities throughout the cyclone were compared with the experimental data and good agreement was verified. The 45 degree angle of the inlet section produced higher values of tangential velocity, mainly for inlet air velocities of 2.75 and 7.75 m/s. The influence was stronger for the low inlet velocities. In Fig. 4, where the inlet gas velocity is 15.2 m/s, the large changes in the tangential velocity profile are not verified. In Fig. 2 a higher swirling velocity, which is about twice the values obtained experimentally without the 45 degree angle, can be observed.

A better representation of tangential velocity for the air inlet velocity of 2.75 m/s can be seen in Fig. 5 (a, b). In both cases the high vorticity preservation phenomenon can be seen. However, for the angled inlet (Fig. 5a), the high tangential velocities can be seen near the cyclone walls and through a large region, while for the conventional design (Fig. 5b), the region of high velocity is not close to the walls and is not as large as it is in the case in Fig. 5a. These characteristics can be important when we analyze gas-solid flow because the solid phase tends to move toward the wall and improve collection efficiency. The other gas inlet velocities used in this work (2.75 and 7.75 m/s) showed the same profile as that shown in Fig. 5.

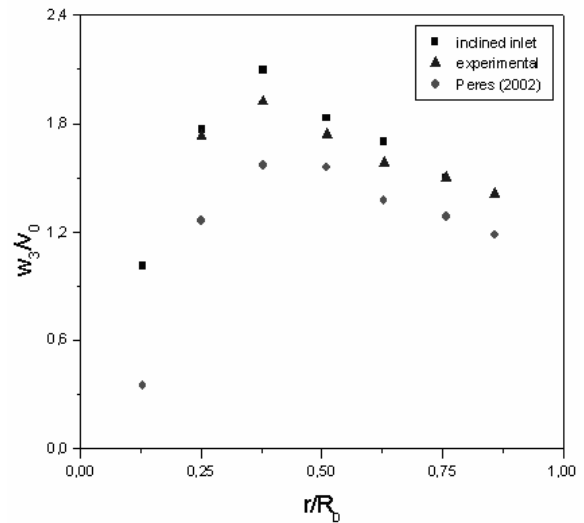


Figure 4. Distributions of tangential velocity in the cyclone ( $v_0 = 15.2$  m/s).

### Gas-Solid Flow

Numerical results for the influence of the cyclone inlet section geometry with a 45 degree angle in relation to the equipment were obtained for the inlet gas-solid velocities (2.75, 7.75 and 15.2 m/s). Figure 6 shows the current numerical results for the distributions of tangential velocity of the gas obtained at a height of 0.12 m from the top of the cylindrical cyclone body.

Figure 6 shows the influence of solids on gas flow on tangential velocities profiles, where it can be seen the decrease of gas tangential velocity peaks for a gas flow with solids. The tangential velocities decreased when the inlet section angle is increased to 45 degrees. This characteristic was observed by Bernardo et al. (2003) and represents a very important characteristic about fluid dynamics of cyclones because there is a relationship between tangential velocity peak and the pressure drop (cyclone performance parameter). For angled inlet cyclones these reductions were about 50%, but this value is higher than the ones obtained using the cyclone without inclined inlet. These results are in agreement with Yuu et al. (1978) and Patterson and Munz (1996). Gas inlet velocity of 2.75 and 7.75 m/s showed the same behavior.

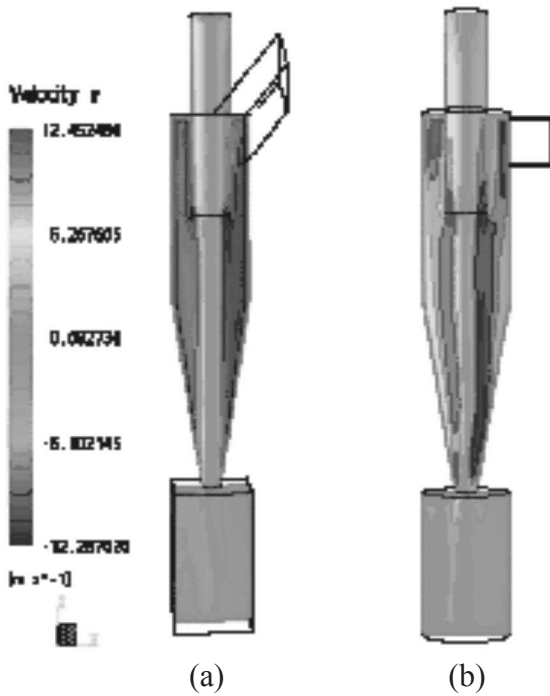


Figure 5. Tangential velocity maps for the numerical solutions: (a) this work, (b) Peres (2002).

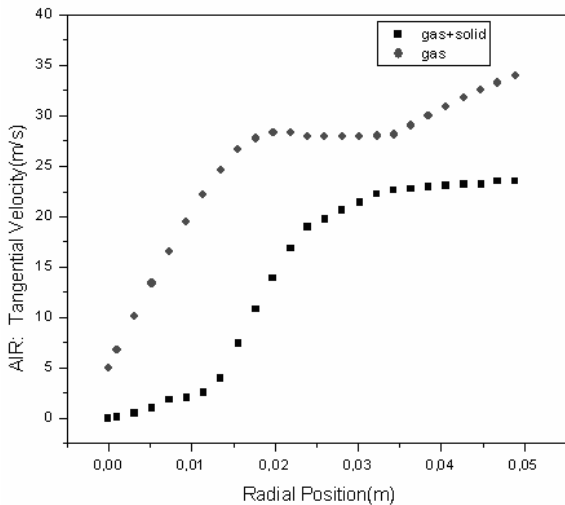


Figure 6. Distribution of gas tangential velocity in gas-solid flow in the cyclone ( $v_0 = 15.2$  m/s).

A better representation of the results for an air inlet velocity of 15.2 m/s can be seen in the maps of velocities (tangential, radial and axial), as shown in Fig. 7. The high tangential velocities can be seen near the cyclone walls (Fig. 7a), in agreement with Fig. 5. Large eddies on reverse flow region and velocities gradients across vertical axes can also be seen. These profiles are in agreement with numerical results obtained by Peres (2002).

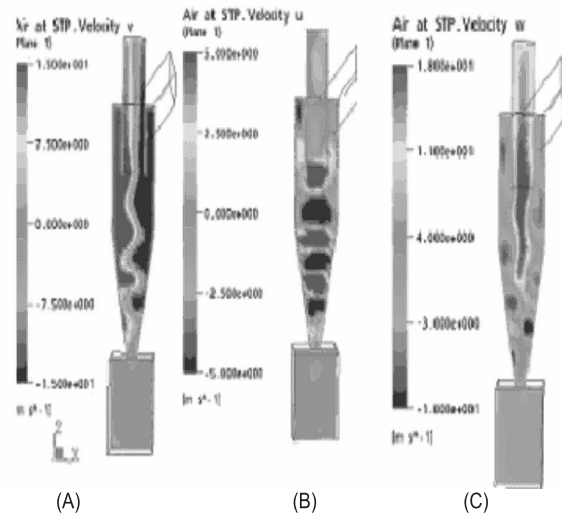


Figure 7. Maps of air velocity in gas-solid flow: (A) tangential, (B) radial and (C) axial.

The method for calculation of the collection efficiency of this cyclone type was based on Meier and Mori (1999). Table 1 shows these results.

Table 1. Performance parameter data.

Performance Parameter	Patterson and Munz (1989)	This work
Collection Efficiency	92%	90.50%
Pressure Drop (PD)	579 Pa	620 Pa
PD Reduction	30%	42%

It can be seen that the performance parameter for this type of cyclone could be obtained with the models. Patterson and Munz (1989) have used the conventional inlet and their results shown in Tab. 1 are only illustrative. The model applied in this study had been previously tested in that work and by Peres (2002). Results showed good agreement with the experimental data of Patterson and Munz (1989), using the cyclone with a normal inlet. Therefore, we conclude that the model was validated and the obtained results are a good representation for this study.

## CONCLUSIONS

The proposal of a new design for the inlet section of the cyclone using a inclination of 45 degrees was analyzed in this work and it was verified that it can be an alternative for increasing the peaks of tangential velocity inside the cyclone without increasing the pressure drop. The influence of the inlet with a 45 degree angle in relation to the equipment in multiphase flows is currently being

performed by our group, and future work describing these effects on collection efficiency will be presented. Regarding the velocity distributions in the gas-solid flow, this modification gave under-predicted values for the gas velocity profile when there were solids in the flow. All results indicate that this proposed 45 degree inlet can provide an alternative for studying the fluid dynamics inside this equipment and increasing performance parameters.

The next step in this work is to apply the angled inlet section in different types of cyclones, specially of the industrial type.

## ACKNOWLEDGEMENTS

The authors are grateful to FAPESP (process number 00/03966-3) for its financial support.

## REFERENCES

Bernardo, S., Peres, A. P., Mori, M. and Huziwar, W.K., 2003, Influence of Inlet section Angle on Cyclones Gas Flow Fluid Dynamics, Proceedings on XXIV CILAMCE – Congresso Ibero Latino-Americano em Métodos Computacionais em Engenharia, Ouro Preto- Brazil.

Crawford, M., 1976, Air pollution control theory, McGraw-Hill.

Dirgo, J., Leith, D., 1985, Performance of theoretically optimized cyclones, Filtration and Separation, March/April, pp. 119-125.

Duggins, R. K., Frith, P. C. W., 1987, Turbulence anisotropy in cyclone, Filtration and Separation, Vol. 24, pp. 394-397.

Hoekstra, A. J., Derksen, J. J. and Van Den Akker, H.E.A., 1999, An Experimental and Numerical Study of Turbulent Swirling Flow in Gas Cyclones, Chemical Engineering Science, Vol. 54, pp. 2055-2065.

Lapple, C. E., 1951, Process use many collectors types, Chemical Engineering, Vol. May, pp. 144-151.

Meier, M., Mori, M., 1999, Anisotropic behavior of the Reynolds stress in gas and gas-solid flows in cyclones, Powder Tech., Vol. 101, pp. 108-119.

Ogawa, A., 1984, Separation of particles from air and gases, I and II, CRC Press, Florida.

Patankar, S. V., 1980, Numerical Heat Transfer and Fluid Flow, Ed. Hemisphere Pub. Co., New York.

Patterson, P. A., Munz, R. J., 1989, Cyclone Collection Efficiencies at very High Temperatures,

The Canadian Journal of Chemical Engineering, Vol. 67, April, pp. 321-328.

Patterson, P. A., Munz, R. J., 1996, Gas and Particle flow patterns at room and elevated temperatures, The Canadian Journal of Chemical Engineering, Vol. 74, April, pp. 213-221.

Peres, A. P., 2002, Estudo experimental e Técnicas de Fluidodinâmica Computacional (CFD) aplicadas a Escoamentos em Ciclones, Doctoral Thesis, UNICAMP, Campinas-SP. (in Portuguese)

Stairmand, C. J., 1951, The design and performance of cyclone separators, Transaction Institute of Chemical Engineering., Vol. 29, pp. 356-373.

Storch, O., 1979, Industrial separators for gas cleaning, Elsevier.

Yuu, S., Jotaki, T., Tomita, Y., Yoshida, K., 1978, The Reduction of Pressure Drop Due to Dust Loading in a Conventional Cyclone, Chemical Engineering Science, Vol. 33, pp. 1573-1580.